

# Unconventional high-temperature ferromagnetic semiconductor

## $\text{PbPd}_{1-x-y}\text{Fe}_y\text{Li}_x\text{O}_2$

Cite as: J. Appl. Phys. **129**, 203903 (2021); <https://doi.org/10.1063/5.0051283>

Submitted: 24 March 2021 • Accepted: 11 May 2021 • Published Online: 26 May 2021

Yangchen He, Daiki Sato, Kazuki Misawa, et al.

### COLLECTIONS

 This paper was selected as an Editor's Pick



View Online



Export Citation



CrossMark

### ARTICLES YOU MAY BE INTERESTED IN

[Local-probe based electrical characterization of a multiphase intermetallic  \$\gamma\$ -TiAl based alloy](#)  
Journal of Applied Physics **129**, 205107 (2021); <https://doi.org/10.1063/5.0048560>

[Polarization induced interface and electron sheet charges of pseudomorphic ScAlN/GaN, GaAlN/GaN, InAlN/GaN, and InAlN/InN heterostructures](#)

Journal of Applied Physics **129**, 204501 (2021); <https://doi.org/10.1063/5.0049185>

[Polar Kerr effect and perpendicular magnetic anisotropy in Fabry-Pérot cavity containing CoPt/AZO magneto-optical interference layer](#)

Journal of Applied Physics **129**, 203902 (2021); <https://doi.org/10.1063/5.0052232>



Applied Physics  
Reviews

Read. Cite. Publish. Repeat.

**19.162**  
2020 IMPACT FACTOR\*

# Unconventional high-temperature ferromagnetic semiconductor $\text{PbPd}_{1-x-y}\text{Fe}_y\text{Li}_x\text{O}_2$

Cite as: J. Appl. Phys. 129, 203903 (2021); doi: 10.1063/5.0051283

Submitted: 24 March 2021 · Accepted: 11 May 2021 ·

Published Online: 26 May 2021



Yangchen He,<sup>a)</sup> Daiki Sato, Kazuki Misawa, Daiki Nishihara, Akinori Kimura, Akitoshi Nakano,<sup>b)</sup> Hiroki Taniguchi,<sup>b)</sup> and Ichiro Terasaki<sup>b)</sup>

## AFFILIATIONS

Department of Physics, Nagoya University, Nagoya 464-8601, Japan

<sup>a)</sup>Also at: HongYi Honor School, Wuhan University, Wuhan 27-430072, China.

<sup>b)</sup>Author to whom correspondence should be addressed: terra@nagoya-u.jp

## ABSTRACT

We have prepared a set of polycrystalline samples of  $\text{PbPd}_{1-x-y}\text{Fe}_y\text{Li}_x\text{O}_2$  ( $x = 0, 0.01, 0.02, 0.03, \text{ and } 0.04$ ;  $y = 0, 0.02, \text{ and } 0.05$ ) and have measured synchrotron x-ray diffraction and magnetization systematically. We have found high-temperature ferromagnetism in Fe- and Li-substituted samples and the largest magnetic moment of  $0.023 \mu_B$  per formula unit in  $\text{PbPd}_{0.93}\text{Fe}_{0.05}\text{Li}_{0.02}\text{O}_2$ . The ferromagnetism survives at 700 K, and the Curie temperature will be far above 800 K. Although similar but controversial high-temperature ferromagnets have been reported in many thin-film samples thus far, the discovered ferromagnetism is macroscopic in the sense that bulk samples stick to a permanent magnet at room temperature. The Fe and Li dependence of the ferromagnetism is complicated, implying that the ferromagnetism is truly unconventional.

Published under an exclusive license by AIP Publishing. <https://doi.org/10.1063/5.0051283>

## I. INTRODUCTION

Ferromagnetism has devoted vital contributions to statistical and condensed-matter physics.<sup>1</sup> This is a prototypical phenomenon for phase transitions, in which Curie and Weiss tried to understand within classical electromagnetism on the assumption of a hypothetical molecular field of tens of tesla. After the advent of quantum mechanics, Heisenberg gave microscopic physical meaning to the molecular field, and now, we regard this as an example of mean field approximation. Landau and his collaborators constructed a phenomenology for ferromagnetism, which is now taken as a first description of symmetry breaking. Even nowadays, the ferromagnetism is still associated with central issues of condensed-matter physics, such as multiferroics (coexistence with ferroelectricity),<sup>2</sup> spintronics (spin-dependent transport),<sup>3,4</sup> and spin caloritics (cross-correlation with heat).<sup>5</sup>

Above all, ferromagnetic semiconductors<sup>6-10</sup> occupy a special position in the physics of ferromagnetism because (1) any free electron systems with low-electron density cannot be ferromagnetic within conventional theories,<sup>11</sup> and thus ferromagnetic semiconductor may break a new ground in condensed-matter physics; (2) ferromagnetism can be controlled by an external electric field and optical absorption,<sup>12</sup> as electric charge is similarly controlled

by such a impetus in conventional semiconductors; and (3) the spin degree of freedom can be controlled to make more efficient and more compact devices for information processing.<sup>13</sup> Since Ohno *et al.* discovered the ferromagnetic semiconductor (Ga,Mn)As in 1996,<sup>14</sup> many researchers have rushed into this area and synthesized many ferromagnetic semiconductors.<sup>15,16</sup> Unfortunately, none of such materials have cleared the criterion proposed by MacDonald *et al.*,<sup>17</sup> and material's development is still going on.

The layered palladium oxide  $\text{PbPdO}_2$  has been investigated as a possible candidate for ferromagnetic semiconductor. This oxide was first synthesized and identified by Meyer and Müller-Buschbaum in the 1970s.<sup>18</sup> The crystal structure of  $\text{PbPdO}_2$  is schematically shown in Fig. 1(c), where  $\text{PdO}_4$  square planes are corner-shared to form the corrugated  $\text{PdO}_2$  plane. The  $\text{PdO}_2$  planes and the Pb layer alternately stack along the *a*-axis direction to make a layered structure with orthorhombic space group *Imma*. The transport properties have been measured rather recently by Ozawa *et al.*<sup>19,20</sup> They have found that the resistivity is metallic around room temperature, takes a broad minimum around 90 K, and shows an upturn toward 0 K. A positive thermopower of  $100 \mu\text{V/K}$  and a positive Hall coefficient of  $10^{-1} \text{ cm}^3/\text{C}$  at 300 K indicate that  $\text{PbPdO}_2$  belongs to hole-doped degenerate

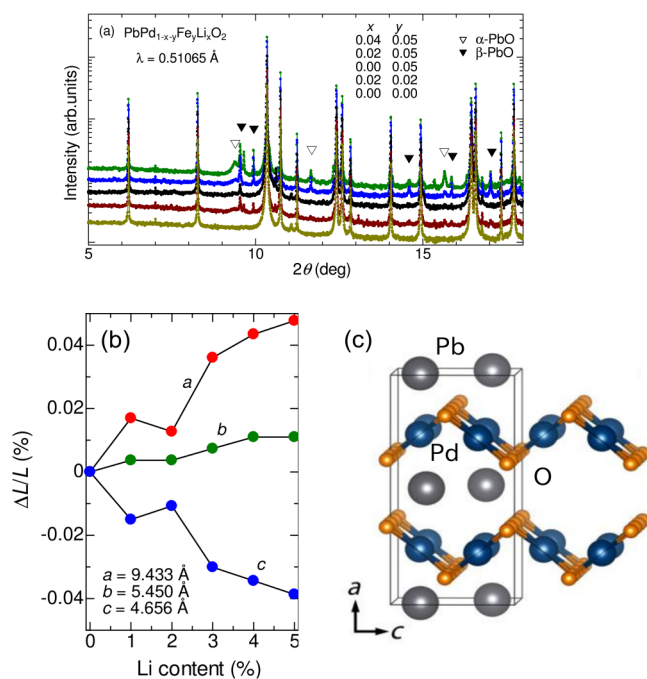


**FIG. 1.** (a) Synchrotron x-ray diffraction patterns of  $\text{PbPd}_{1-x-y}\text{Fe}_y\text{Li}_x\text{O}_2$ . The values of  $x$  and  $y$  are indicated in the legend. Reflections from  $\text{PbO}$  are indicated by open and close triangles ( $\nabla$ ,  $\blacktriangledown$ ). (b) Relative change of the lattice constants with the Li content in  $\text{PbPd}_{0.95-x}\text{Fe}_{0.05}\text{Li}_x\text{O}_2$ . The lattice parameters for  $x = 0$  are given in the legend. (c) Crystal structure of  $\text{PbPdO}_2$ .

semiconductor. After their measurement, Wang<sup>21</sup> has theoretically proposed a new electronic state called spin-gapless semiconductor in Co-doped  $\text{PbPdO}_2$ . According to his proposal, a high-temperature ferromagnetic semiconductor can be designed, where holes and electrons are fully polarized. Motivated by his prediction, many experimental research studies using polycrystalline samples<sup>22–24</sup> and film samples<sup>25–29</sup> have been carried out. However, no obvious experimental evidence for spin-gapless semiconductor has been confirmed.

We have studied palladium-based oxides to explore novel properties. Palladium oxides are known to have unique crystal structures composed of the square planar  $\text{PdO}_4$  block.<sup>30</sup> The Pd ion is formally divalent, and the electronic configuration is  $t_{2g}^6 d_{z^2}$ . Accordingly, one can expect a small energy gap between  $d_{z^2}$  and  $d_{x^2-y^2}$ .<sup>31</sup> Ichikawa *et al.*<sup>32,33</sup> reported that Li substitution for Pd in  $\text{CaPd}_3\text{O}_4$  makes p-type thermoelectric materials, and Bi substitution for Ca makes n-type thermoelectric oxides. Shibasaki and Terasaki<sup>34</sup> studied the thermoelectric properties of the layered palladate  $R_2\text{PdO}_4$  ( $R = \text{La}, \text{Nd}, \text{Sm}, \text{and Gd}$ ). Terasaki *et al.*<sup>35</sup> synthesized a solid solution of  $\text{CaPd}_{3-x}\text{Cu}_x\text{O}_4$ , in which a unique three-dimensional  $\text{CuO}_4$  network is realized. Here, we report the magnetic properties of  $\text{PbPd}_{1-x-y}\text{Fe}_y\text{Li}_x\text{O}_2$  and find that the co-doping of Li and Fe turns this oxide into a high-temperature ferromagnetic semiconductor. This ferromagnetism is unprecedented and highly unconventional, and we expect that it will pave a new way to ferromagnetism.

## II. EXPERIMENTAL

A set of polycrystalline samples of  $\text{PbPd}_{1-x-y}\text{Fe}_y\text{Li}_x\text{O}_2$  ( $x = 0, 0.01, 0.02, 0.03, \text{and } 0.04$ ;  $y = 0, 0.02, \text{and } 0.05$ ) were prepared with the standard solid-state reaction method. Stoichiometric amounts of high purity powders of PdO (99.9%), PbO (99.999%),  $\text{Li}_2\text{CO}_3$  (99.9%), and  $\alpha\text{-Fe}_2\text{O}_3$  (99.99%) were ground in an agate mortar with an agate pestle and were pressed into pellets at 20 MPa. The pellets were sintered in  $\text{Al}_2\text{O}_3$  flat crucibles for 48 h at 720 °C in air. As a reference, another set of polycrystalline samples of  $\text{Pb}_{1-x}\text{Ag}_x\text{Pd}_{0.95}\text{Fe}_{0.05}\text{O}_2$  ( $x = 0, 0.05, \text{and } 0.10$ ) were prepared with the same procedure using PdO (99.9%), PbO (99.999%),  $\text{Ag}_2\text{O}$  (99.9%), and  $\alpha\text{-Fe}_2\text{O}_3$  (99.99%). Since Li is difficult to detect in x-ray diffraction, we use the nominal composition throughout this paper.

Synchrotron x-ray-diffraction (SXRD) data were collected with a wavelength of 0.510 65 Å on an imaging plate using a large Debye-Scherrer camera installed at BL02B2, SPring-8.<sup>36</sup> A well-ground polycrystalline sample was sealed into a glass capillary with an internal diameter of 0.2 mm. Magnetization ( $M$ ) was measured using a SQUID susceptometer (Quantum Design, MPMS) with the high-temperature option above 350 K. The temperature dependence of the magnetization was measured in 0.1 T in a field-heating process after zero-field cooling. The magnetization-field ( $M$ - $H$ ) curves were taken in sweeping magnetic fields from  $-7$  to 7 T. The magnetic relaxation was recorded as a function of time after field cooling at 0.1 T down to 10 K, followed by a rapid quench down to 0 T in 200 s.

## III. RESULTS AND DISCUSSION

Figure 1(a) shows typical SXRD patterns for  $\text{PbPd}_{1-x-y}\text{Fe}_y\text{Li}_x\text{O}_2$  on a semi-log scale, where the baselines are properly shifted for clarity. Almost all the diffraction peaks are indexed as  $\text{PbPdO}_2$  except for a tiny trace of  $\text{PbO}$  as marked with  $\nabla$  and  $\blacktriangledown$ ,<sup>37</sup> indicating that Fe and Li are successfully substituted for Pd. The peak intensities of  $\text{PbO}$  impurity phase increase with Li concentration  $x$ . Lamontagne *et al.*<sup>38</sup> synthesized  $\text{PbPd}_{1-x}\text{Li}_x\text{O}_2$  and reported that  $\text{PbO}$  appeared as impurity for  $x > 0.08$ . We will discuss the relationship of the impurity fraction evaluated through the Rietveld refinement to the intrinsic properties of this compound below.

From the diffraction patterns, we obtain the lattice constants of  $\text{PbPdO}_2$  to be  $a = 9.433$  Å,  $b = 5.450$  Å, and  $c = 4.656$  Å, which are consistent with the literature.<sup>19,38</sup> Figure 1(b) shows the relative change in the lattice parameters plotted as a function of the Li content  $x$  in  $\text{PbPd}_{0.95-x}\text{Fe}_{0.05}\text{Li}_x\text{O}_2$ . All the lattice constants systematically change with  $x$ , indicating that the Li ions are successfully substituted. Since  $\text{Li}^+$  ion is much smaller (0.59 Å) than  $\text{Pb}^{2+}$  (1.2 Å) ion, it unlikely enters the Pb site. Even if it entered, all the lattice parameters would significantly decrease with  $x$ . This speculation is inconsistent with Fig. 1(b). Lamontagne *et al.*<sup>38</sup> discussed a possibility that Li might have occupied the Pb site but came to the conclusion that Li was unlikely to enter the Pb site from the bond-valence sum analysis. Following their analysis, we also concluded that Li was successfully substituted the Pd ion and also regarded that the oxygen content was stoichiometric.

Figure 2(a) shows the magnetization-field curves of  $\text{PbPd}_{0.95-x}\text{Fe}_{0.05}\text{Li}_x\text{O}_2$  ( $x = 0$  and 0.02). For  $x = 0.00$ , the

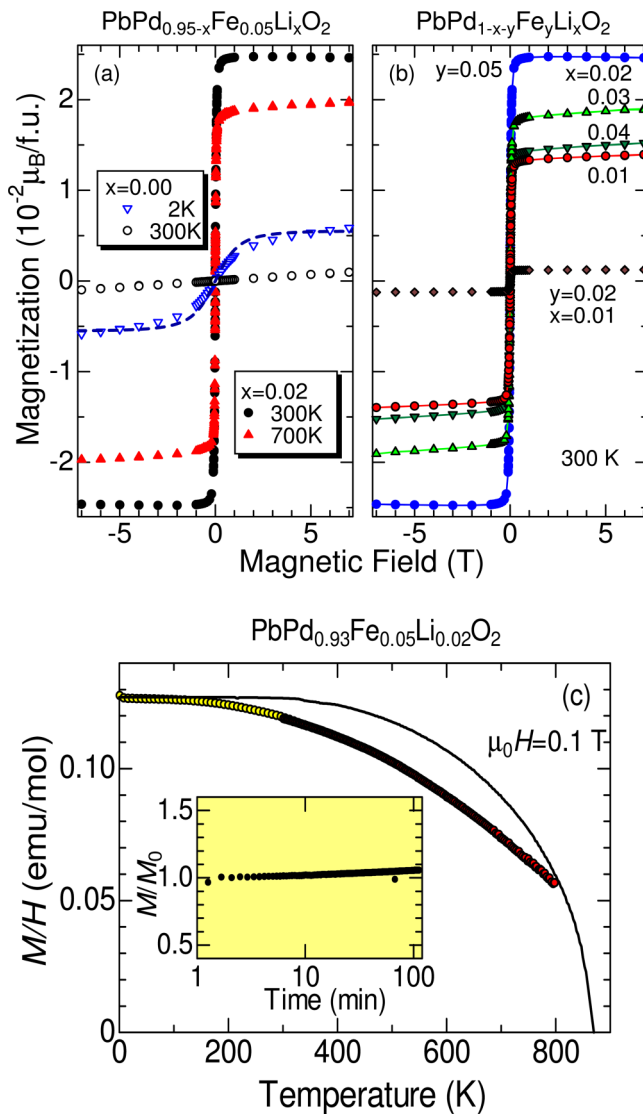


**FIG. 2.** (a) Magnetization-field ( $M-H$ ) curves for  $\text{PbPd}_{0.95-x}\text{Fe}_{0.05}\text{Li}_x\text{O}_2$  ( $x = 0$  and  $0.02$ ) for various temperatures. The dotted curve represents the Brillouin function for  $J = 5/2$  (see text). (b) Room temperature  $M-H$  curves for  $\text{PbPd}_{1-x-y}\text{Fe}_y\text{Li}_x\text{O}_2$ . (c) Magnetization of  $\text{PbPd}_{0.93}\text{Fe}_{0.05}\text{Li}_{0.02}\text{O}_2$  plotted as a function of temperature in  $0.1\text{ T}$ . The data were independently measured below and above  $350\text{ K}$ , in which the high-temperature data were normalized to the low-temperature data. The solid curve represent the theoretical curve for molecular field approximation with  $T_c = 860\text{ K}$ . The inset shows the magnetization relaxation taken at  $10\text{ K}$  after a field cooling of  $0.1\text{ T}$ .

magnetization is linear in  $H$  at  $300\text{ K}$ , showing that the  $x = 0$  sample ( $\text{PbPd}_{0.95}\text{Fe}_{0.05}\text{O}_2$ ) is paramagnetic, although  $5\%$  Fe ions are introduced in the Pd site. At  $2\text{ K}$ , the magnetization shows non-linear behavior, which can be understood in terms of unwanted magnetic impurity. As is written in textbooks,<sup>1,39</sup> the magnetization

from dilute independent magnetic impurities  $M_{\text{imp}}$  is expressed by

$$M_{\text{imp}} = n_{\text{imp}} g \mu_B J B_J \left( \frac{g \mu_B J \mu_0 H}{k_B T} \right), \quad (1)$$

where  $n_{\text{imp}}$  is the impurity density,  $\mu_B$  is the Bohr magneton, and  $J$  is the total spin number of the impurity.  $B_J$  is the Brillouin function expressed by

$$B_J(x) = \frac{2J+1}{2J} \coth\left(\frac{2J+1}{2J}x\right) - \frac{1}{2J} \coth\left(\frac{1}{2J}x\right). \quad (2)$$

Assuming  $J = 5/2$  and the  $g$ -factor of  $g = 2$ , we find that  $n_{\text{imp}} = 0.0011$  explains the measurement data well, as shown by the dotted curve. This means that around  $0.11\%$  of free  $\text{Fe}^{3+}$  ions per formula unit are present in undetectable impurity phases. A similar but simpler evaluation is to translate the  $7\text{-T}$  magnetization into the concentration of  $\text{Fe}^{3+}$  spins. A value of  $5.5 \times 10^{-3} \mu_B/\text{f.u.}$  corresponds to  $1.1 \times 10^{-3}/\text{f.u.}$  for  $gJ = 5\mu_B$ . Although other possibilities such as  $\text{Fe}^{2+}$  impurity phase cannot be ruled out, the corresponding impurity concentration is as small as  $0.1\%$ . Such a small concentration is comparable with the purity of  $\text{LiCO}_3$  and  $\text{PbO}$  powders. The Fe ions in impurity oxide phases usually exist as the high-spin state, and the above estimation is most probable. At the same time, it means that Fe ions incorporated in  $\text{PbPdO}_2$  behave almost nonmagnetic, as is discussed later.

Most unexpectedly, *the nonmagnetic Li substitution drives the samples to be ferromagnetic.* The saturation magnetization  $M_s$  is clearly observed at  $300$  and  $700\text{ K}$  for  $x = 0.02$ , demonstrating high-temperature ferromagnetism in this compound. No hysteresis is visible, showing that this ferromagnet is soft with a tiny coercive field ( $\sim 4\text{ mT}$ ).  $M_s$  at  $300\text{ K}$  is around  $0.023 \mu_B$  per formula unit, suggesting that  $1.15 \mu_B$  is generated per Li ion. At  $700\text{ K}$ ,  $M_s$  somewhat decreases, but the soft-magnet behavior remains intact even at this high temperature. Owing to the experimental limitations, we failed in measuring the transition temperature of this compound, which must be far above  $800\text{ K}$ . The carrier concentration is evaluated to be  $1 \times 10^{19}\text{ cm}^{-3}$  from the Hall coefficient. This low value cannot explain such high Curie temperature from the Zener model.<sup>40</sup>

We should emphasize that the present study is the first and unambiguous observation of ferromagnetism in  $\text{PbPdO}_2$ -related materials. Jung and the collaborators reported the non-linear  $M-H$  at  $2\text{ K}$  for samples doped with Co,<sup>22,23</sup> Cu,<sup>24</sup> and Zn,<sup>24</sup> which may come from free magnetic impurity as we discussed in  $\text{PbPd}_{0.95}\text{Fe}_{0.05}\text{O}_2$ . Su *et al.* showed high-temperature ferromagnetism in nano-grain film samples with Fe,<sup>28</sup> Co,<sup>26</sup> and Ni doping,<sup>29</sup> but the magnetic signal was as small as  $10^{-6}\text{ emu}$ , in which a possibility of unwanted contamination cannot be excluded as is similar to other oxide ferromagnetic semiconductors.<sup>41</sup> We emphasize that this high-temperature ferromagnetism is observed in bulk samples, and this large magnetization is macroscopic in the sense that ceramic samples of  $\text{PbPd}_{0.93}\text{Fe}_{0.05}\text{Li}_{0.02}\text{O}_2$  stick to a permanent magnet at room temperature.

Figure 2(c) shows  $M/H$  for  $\text{PbPd}_{0.93}\text{Fe}_{0.05}\text{Li}_{0.02}\text{O}_2$  in  $0.1\text{ T}$  plotted as a function of temperature in the field-cooling (FC) process. The  $M/H$  data after the zero-field cooling are almost

identical to the FC data owing to the soft magnetic nature (not shown). For the high-temperature measurement above 350 K, we used the high-temperature measurement option in MPMS. The high-temperature data were normalized to the low-temperature data to be connected smoothly. As we saw in the  $M-H$  curve in Fig. 2(a), the sample shows a large magnetization at 700 K and continues to show a large signal up to 800 K. We notice that the temperature dependence is more moderate than the prediction from the molecular field approximation. The solid curve represents the magnetization calculated from the molecular field approximation with  $T_c = 860$  K, but it cannot explain the observed data well. This suggests that the observed ferromagnetism should arise from unconventional origin. This gradual growth of the magnetization may come from ferromagnetic nano-size impurities distributed inhomogeneously with a wide variation of the Curie temperature. We can exclude such possibilities by looking at the  $M-H$  curves in Fig. 2(a). If inhomogeneous nano-size impurities were present, the magnetization would not saturate at a small field of  $\sim 0.1$  T and continue to increase with  $H$ .

The inset in Fig. 2(c) shows the magnetization relaxation at 10 K. The sample was cooled down in 0.1 T from 300 K, and the field was quenched at a speed of  $5 \times 10^{-4}$  T/s at 10 K. As seen in this figure, the large magnetization stays constant, or even slightly increases, excluding a possibility of superparamagnetism or spin-glass-like state. We note that the coercive field ( $\sim 4$  mT) is small but almost independent of temperature, which is difficult to explain from simple superparamagnetism. We do not understand the slight increase of the magnetization, and suffice it to say that this may come from the imperfect experimental condition that the sample was not heated up above  $T_c$ .

The ferromagnetism shows complicated composition dependence. Figure 2(b) shows the room temperature magnetization for various samples. All the data obviously show soft-magnet-like field dependence, indicating that all the samples are ferromagnetic at room temperature.  $M_s$  for  $y = 0.05$  increases with the Li content from  $x = 0.01$  to 0.02, and then turns to decrease from 0.02 to 0.04. As was shown in Fig. 1(a), the PbO impurity increased with  $x$ . If the ferromagnetic behavior were due to impurities, the saturation magnetization would increase with  $x$ .  $M_s$  of  $x = 0.01$  for  $y = 0.02$  is much smaller than  $M_s$  of  $x = 0.01$  for  $y = 0.05$ . This indicates that proper contents of Fe and Li ions are indispensable to the high-temperature ferromagnetism.

Let us discuss a possibility that the high-temperature ferromagnetism observed in the present samples might have come from unwanted impurity phases. We pay a special attention to the relationship of the impurity fraction to the saturation magnetization, for our sample includes a tiny fraction of PbO impurities. Figure 3(a) shows the x-ray diffraction patterns of  $\text{PbPd}_{0.95-x}\text{Fe}_{0.05}\text{Li}_x\text{O}_2$  on a linear scale, in order to clearly see the peak intensity ( $9.54^\circ$  and  $9.95^\circ$ ) of PbO phases, where the solid curve represents the Rietveld refinement with multiple phases. In the inset, the PbO impurity peaks are shown in a magnified view. From this figure, one can see that the impurity fraction is almost the same between  $x = 0.00$  and 0.01, while the former sample is paramagnetic and the latter ferromagnetic with  $M_s = 1.5 \mu_B$  per Li. This naturally indicates that the PbO impurity has nothing to do with the occurrence of high-temperature ferromagnetism.

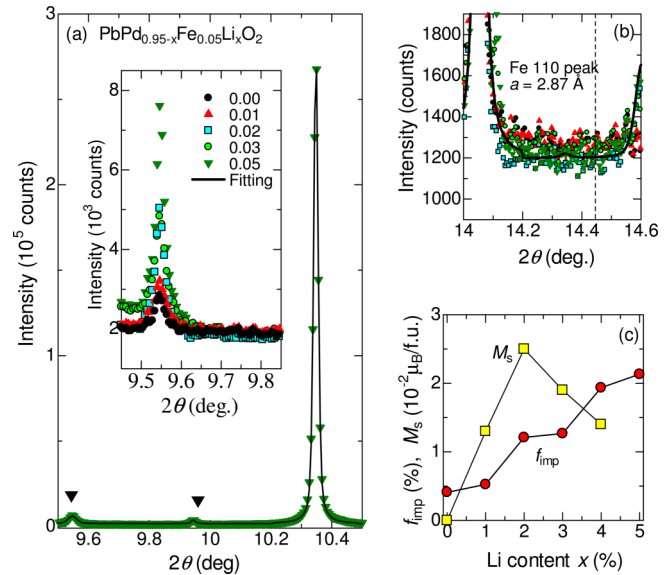


**FIG. 3.** (a) The XRD pattern of  $\text{PbPd}_{0.95-x}\text{Fe}_{0.05}\text{Li}_x\text{O}_2$ . The solid curve represents the Rietveld refinement with multiple phases. The inset shows the magnified view near the PbO reflections. (b) The x-ray intensity near  $2\theta = 14.4^\circ$ . The dotted line represents the position of the main peak of Fe metal. Within the experimental accuracy, no trace of Fe impurity is seen. (c) The impurity fraction  $f_{\text{imp}}$  and the saturation moment  $M_s$  are plotted as a function of Li content  $x$ .

The most suspicious impurity is ferromagnetic Fe metal; other elements of Pb, Pd, and Li are paramagnetic, and no compounds of any combinations are known to be ferromagnetic at 700 K. Since our samples are bulk, the magnetic signal is so large that an upper limit of the fraction of Fe metal can be evaluated. The largest magnetic signal was measured to be 0.09 emu for  $x = 0.02$  at 300 K, and actually, this sample sticks to a permanent magnet at room temperature. This is typically 1000 times larger than that of ferromagnetic thin films.<sup>26,28,29</sup> If the Fe metal showed this signal, its mass would be  $0.09 \text{ emu} / 220 \text{ emu g}^{-1} = 0.4 \text{ mg}$ . The 0.4 mg of Fe corresponds to around 1 mass% of the sample (6 mol.% of the sample), which could be detected in the x-ray diffraction patterns. Figure 3(b) shows a magnified view of the x-ray diffraction patterns of the same samples in Fig. 3(a). If there were ferromagnetic Fe metal in the samples, it would have a main peak of (110) near  $2\theta = 14.45^\circ$ . As shown by the dotted line in this figure, there is no trace of such peak, indicating that the portion of Fe metal is evaluated to be less than the SXR resolution (less than the intensity ratio of  $10^{-4}$ ). In the first place, the samples were sintered at the low temperature of  $700^\circ\text{C}$  in air; such sintering conditions work as oxidizing atmosphere for transition-metal oxides on the basis of the so-called “Ellingham diagram,”<sup>42</sup> and iron oxides are highly unlikely reduced to be Fe metals.

A second suspicious impurity is ferrimagnetic  $\text{Fe}_3\text{O}_4$ . No trace of  $\text{Fe}_3\text{O}_4$  is seen in the x-ray diffraction patterns, and the observed magnetization is significantly larger than the value when all the substituted Fe ions form  $\text{Fe}_3\text{O}_4$ . In addition, the magnetization would show a kink at the Verwey transition temperature of

125 K.<sup>43</sup> Yet another possibility is the precipitation of ferromagnetic Pd–Fe or Pb–Fe alloys. For Pd–Fe alloys, the saturation magnetization (50 emu/g) was four times smaller than that of ferromagnetic iron.<sup>44</sup> Using the same argument above, the fraction of such magnetic impurity is evaluated to be 4 mass% of the sample. Such a large fraction should be detected in SXRD. Even if the precipitation were far smaller in size than the SXRD resolution, such ferromagnetic nanoparticle would show superparamagnetism, which is not the present case as shown in the inset of Fig. 2(c). For the Pb–Fe alloy, Pb and Fe construct a famous immiscible system, and such an alloy is unlikely to show up in thermal equilibrium conditions.<sup>45</sup>

Figure 3(c) shows  $M_s$  and the impurity fraction  $f_{\text{imp}}$  evaluated from the Rietveld refinement plotted as a function of  $x$ . Although the impurity fraction almost linearly increases with  $x$ ,  $M_s$  shows a peak at  $x = 0.02$ . This further consolidates our conclusion that the impurity phase has no correlation with the high-temperature ferromagnetism.

Finally, we find that Li substitution is not always indispensable to high-temperature ferromagnetism. We have observed a similar ferromagnetism in  $\text{Pb}_{1-x}\text{Ag}_x\text{Pd}_{0.95}\text{Fe}_{0.05}\text{O}_2$ , where  $\text{Ag}^{1+}$  substitutes for  $\text{Pb}^{2+}$  in the Pb layer to supply holes. Figure 4 shows the magnetic susceptibility evaluated by  $M/H$  for  $\text{Pb}_{1-x}\text{Ag}_x\text{Pd}_{0.95}\text{Fe}_{0.05}\text{O}_2$  ( $x = 0, 0.05, \text{ and } 0.10$ ) measured in 0.1 T. For comparison, we also show the susceptibility of  $\text{PbPdO}_2$  measured in 7 T. As was already discussed, the  $x = 0$  sample is paramagnetic with a slight upturn of

Curie tail with 0.1% of  $J = 5/2$  independent spins. The solid curve represents the fitting curve with the Curie law expressed by

$$\chi = \frac{C}{T} + \chi_0, \quad (3)$$

where  $C$  is the Curie constant and  $\chi_0$  the temperature-independent susceptibility. The fitting is satisfactory with  $C = 0.0073$  emu K/mol, and  $\chi_0 = 1.1 \times 10^{-4}$  emu/mol. The Curie constant is further written by  $C = n_{\text{imp}}(\mu_{\text{eff}})^2/3k_B = n_{\text{imp}}(g\mu_B)^2S(S+1)/3k_B$ , where  $n_{\text{imp}}$  is the impurity density for the Curie tail and  $\mu_{\text{eff}}$  is the effective magnetic moment. We obtain  $\mu_{\text{eff}} = 6.8\mu_B$  assuming that  $n_{\text{imp}} = 0.0011$  obtained from the  $M-H$  curve at 2 K. This is close to, or slightly larger than the value for  $J = 5/2$  ( $5.5\mu_B$ ), suggesting that around 0.1% of free  $\text{Fe}^{3+}$  ions are responsible for the Curie tail. This means that the Fe ions in  $\text{PbPd}_{0.95}\text{Fe}_{0.05}\text{O}_2$  show small and temperature-independent susceptibility  $\chi_0$ . One reasonable explanation for this is that the substituted Fe ions are in the low-spin state ( $S = 0$  for  $\text{Fe}^{2+}$  or  $S = 1/2$  for  $\text{Fe}^{3+}$ ). Although Fe ions are usually stable as the high-spin state in transition-metal oxides, we yet think the low-spin state plausible, for the Pd ion is surrounded by a planer oxygen square that causes a strong two-dimensional ligand field. As a preliminary result, a single crystal of  $\text{PbPd}_{0.95}\text{Fe}_{0.05}\text{O}_2$  shows almost temperature-independent susceptibility, which implies weak magnetic behavior of the substituted Fe ions. The valence and spin state of the Fe ion in  $\text{PbPdO}_2$  are to be determined by further studies.

With Ag substitution, susceptibility rapidly grows as large as  $10^{-2}$  emu/mol. The inset shows the  $M-H$  curves at 20 K, in which  $M$  is clearly nonlinear in  $H$ . These data show that the ground state of  $x = 0.05$  and  $0.10$  is ferromagnetic, as is similar to the Li-substituted samples. In  $\text{Pb}_{1-x}\text{Ag}_x\text{Pd}_{0.95}\text{Fe}_{0.05}\text{O}_2$  and  $\text{PbPd}_{0.95-x}\text{Fe}_{0.05}\text{Li}_x\text{O}_2$ , co-doping effect provokes high-temperature ferromagnetism, and nonmagnetic acceptors play a vital role in the ferromagnetism. However, we should mention that the ferromagnetism is quantitatively different between the two systems. 2% Li can induce a large magnetic moment of  $1.2\mu_B$  per Li in  $\text{PbPd}_{0.95-x}\text{Fe}_{0.05}\text{Li}_x\text{O}_2$ , while 10% Ag induces only  $0.05\mu_B$  per Ag in  $\text{Pb}_{1-x}\text{Ag}_x\text{Pd}_{0.95}\text{Fe}_{0.05}\text{O}_2$ .

#### IV. SUMMARY

In summary, we have prepared a set of polycrystalline samples of  $\text{PbPd}_{1-x-y}\text{Fe}_y\text{Li}_x\text{O}_2$  and measured the synchrotron x-ray diffraction patterns and the magnetic properties systematically. We have discovered that the Fe-substituted samples  $\text{PbPd}_{1-y}\text{Fe}_y\text{O}_2$  are paramagnetic without any sign of phase transitions and that the co-substituted samples of Fe and Li show high-temperature ferromagnetism below 800 K. The largest saturation moment at 300 K was obtained to be  $0.023\mu_B$  per formula unit or  $1.15\mu_B$  per Li for  $x = 0.02$  and  $y = 0.05$ . Careful analysis has revealed that the observed ferromagnetic signal is too strong to be assigned to extrinsic magnetic contamination and or impurity phases. Microscopic mechanism for the high-temperature ferromagnetism should be clarified by further studies including first-principle calculation. In particular, the valence and spin state of the Fe ions substituted in the  $\text{PbO}_4$  plane need to be determined experimentally.

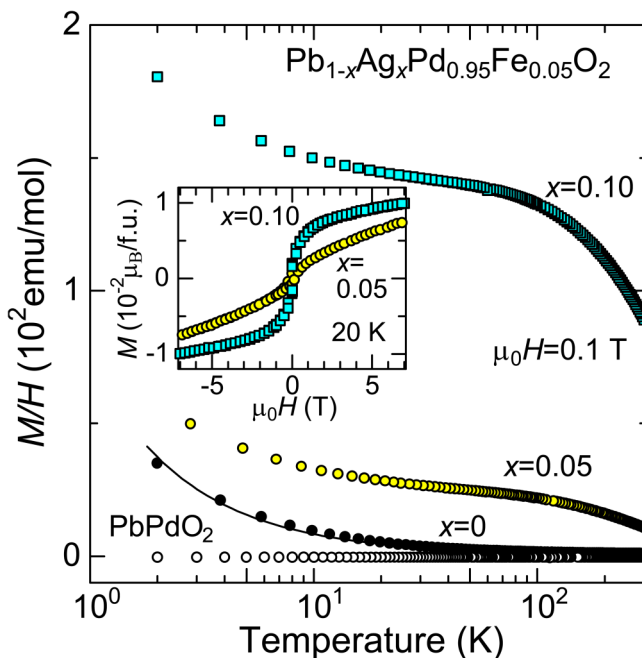


**FIG. 4.** Magnetization divided by the external field of 0.1 T for  $\text{Pb}_{1-x}\text{Ag}_x\text{Pd}_{0.95}\text{Fe}_{0.05}\text{O}_2$  is plotted as a function of temperature. The susceptibility of  $\text{PbPdO}_2$  measured in 7 T is also plotted for comparison. The solid curve is the result of the Curie fitting assuming the impurity density of 0.1% (see text). The inset shows the magnetization-field curves for  $x = 0.05$  and  $0.10$  at 20 K.

## ACKNOWLEDGMENTS

The authors would like to thank S. Inagaki, K. Kawamura, and T. D. Yamamoto for collaboration at an early stage of this study and also thank T. Taniyama for carefully reading our manuscript and giving useful comments to us. This study was partially supported by Grant-in-Aid for Scientific Research (Kakenhi Nos. 15K13519, 19H05791, and 20K20898) by MEXT. The synchrotron radiation experiments at the BL02B2 beamline of the SPring-8 facility were conducted with the approval of the Japan Synchrotron Radiation Research Institute (JASRI) (Proposal No. 2019B1089). Y.H. would like to acknowledge the scholarships for abroad study from Wuhan University.

## DATA AVAILABILITY

The data that support the findings of this study are available from the corresponding author upon reasonable request.

## REFERENCES

- <sup>1</sup>R. M. White, *Quantum Theory of Magnetism* (Springer, Berlin, 2007).
- <sup>2</sup>S.-W. Cheong and M. Mostovoy, *Nat. Mater.* **6**, 13 (2007).
- <sup>3</sup>S. Bader and S. Parkin, *Ann. Rev. Condens. Matter Phys.* **1**, 71 (2010).
- <sup>4</sup>A. Hoffmann and S. D. Bader, *Phys. Rev. Appl.* **4**, 047001 (2015).
- <sup>5</sup>G. E. W. Bauer, E. Saitoh, and B. J. van Wees, *Nat. Mater.* **11**, 391 (2012).
- <sup>6</sup>H. Ohno, *Science* **281**, 951 (1998).
- <sup>7</sup>T. Dietl, *Semicond. Sci. Technol.* **17**, 377 (2002).
- <sup>8</sup>K. Ando, *Science* **312**, 1883 (2006).
- <sup>9</sup>S. Kuroda, N. Nishizawa, K. Takita, M. Mitome, Y. Bando, K. Osuch, and T. Dietl, *Nat. Mater.* **6**, 440 (2007).
- <sup>10</sup>K. Sato, L. Bergqvist, J. Kudrnovský, P. H. Dederichs, O. Eriksson, I. Turek, B. Sanyal, G. Bouzerar, H. Katayama-Yoshida, V. A. Dinh, T. Fukushima, H. Kizaki, and R. Zeller, *Rev. Mod. Phys.* **82**, 1633 (2010).
- <sup>11</sup>D. Pines, *Phys. Rev.* **92**, 626 (1953).
- <sup>12</sup>T. Dietl and H. Ohno, *Rev. Mod. Phys.* **86**, 187 (2014).
- <sup>13</sup>D. D. Awschalom and M. E. Flatté, *Nat. Phys.* **3**, 153 (2007).
- <sup>14</sup>H. Ohno, A. Shen, F. Matsukura, A. Oiwa, A. Endo, S. Katsumoto, and Y. Iye, *Appl. Phys. Lett.* **69**, 363 (1996).
- <sup>15</sup>M. L. Reed, N. A. El-Masry, H. H. Stadelmaier, M. K. Ritums, M. J. Reed, C. A. Parker, J. C. Roberts, and S. M. Bedair, *Appl. Phys. Lett.* **79**, 3473 (2001).
- <sup>16</sup>J. M. D. Coey, M. Venkatesan, and C. B. Fitzgerald, *Nat. Mater.* **4**, 173 (2005).
- <sup>17</sup>A. H. MacDonald, P. Schiffer, and N. Samarth, *Nat. Mater.* **4**, 195 (2005).
- <sup>18</sup>H. Meyer and H. Müller-Buschbaum, *Z. Anorg. Allg. Chem.* **442**, 26 (1978).
- <sup>19</sup>T. C. Ozawa, T. Taniguchi, Y. Nagata, Y. Noro, T. Naka, and A. Matsushita, *J. Alloys Compd.* **388**, 1 (2005).
- <sup>20</sup>T. C. Ozawa, T. Taniguchi, Y. Nagata, Y. Noro, T. Naka, and A. Matsushita, *J. Alloys Compd.* **395**, 32 (2005).
- <sup>21</sup>X. L. Wang, *Phys. Rev. Lett.* **100**, 1 (2008).
- <sup>22</sup>K. J. Lee, S. M. Choo, J. B. Yoon, K. M. Song, Y. Saiga, C. Y. You, N. Hur, S. I. Lee, T. Takabatake, and M. H. Jung, *J. Appl. Phys.* **107**, 09C306 (2010).
- <sup>23</sup>K. J. Lee, S. M. Choo, Y. Saiga, T. Takabatake, and M. H. Jung, *J. Appl. Phys.* **109**, 07C316 (2011).
- <sup>24</sup>K. Lee, S. M. Choo, and M. H. Jung, *Appl. Phys. Lett.* **106**, 072406 (2015).
- <sup>25</sup>X. Wang, G. Peleckis, C. Zhang, H. Kimura, and S. Dou, *Adv. Mater.* **21**, 2196 (2009).
- <sup>26</sup>H. L. Su, S. Y. Huang, Y. F. Chiang, J. C. Huang, C. C. Kuo, Y. W. Du, Y. C. Wu, and R. Z. Zuo, *Appl. Phys. Lett.* **99**, 102508 (2011).
- <sup>27</sup>S. M. Choo, K. J. Lee, S. M. Park, G. S. Park, and M. H. Jung, *J. Appl. Phys.* **113**, 014904 (2013).
- <sup>28</sup>J. Liu, C. Mei, P. Y. Chuang, T. T. Song, F. L. Tang, H. L. Su, J. C. Huang, and Y. C. Wu, *Ceram. Int.* **42**, 15762 (2016).
- <sup>29</sup>C. Mei, J. Liu, P. Chuang, T. Song, F. Tang, H. Su, J. Huang, and Y. Wu, *Ceram. Int.* **43**, 1997 (2017).
- <sup>30</sup>R. V. Panin, N. R. Khasanova, A. M. Abakumov, E. V. Antipov, G. V. Tendeloo, and W. Schnelle, *J. Solid State Chem.* **180**, 1566 (2007).
- <sup>31</sup>M. L. Doublet, E. Canadell, and M. H. Whangbo, *J. Am. Chem. Soc.* **116**, 2115 (1994).
- <sup>32</sup>S. Ichikawa and I. Terasaki, *Phys. Rev. B* **68**, 233101 (2003).
- <sup>33</sup>I. Terasaki, S. Ichikawa, and S. Shibusaki, in *Proceedings of the 23rd International Conference on Thermoelectrics (ICT2004)* (IEEE, 2005), p. 094.
- <sup>34</sup>S. Shibusaki and I. Terasaki, *J. Phys. Soc. Jpn.* **75**, 024705 (2006).
- <sup>35</sup>I. Terasaki, K. Misawa, K. Tanabe, and H. Taniguchi, *J. Phys. Soc. Jpn.* **87**, 104603 (2018).
- <sup>36</sup>E. Nishibori, M. Takata, K. Kato, M. Sakata, Y. Kubota, S. Aoyagi, Y. Kuroiwa, M. Yamakata, and N. Ikeda, *J. Phys. Chem. Solids* **62**, 2095 (2001).
- <sup>37</sup>R. Stillman, R. Robins, and M. Skyllas-Kazacos, *J. Power Sources* **13**, 171 (1984).
- <sup>38</sup>L. K. Lamontagne, G. Laurita, M. W. Gaultois, M. Knight, L. Ghadbeigi, T. D. Sparks, M. E. Gruner, R. Pentcheva, C. M. Brown, and R. Seshadri, *Chem. Mater.* **28**, 3367 (2016).
- <sup>39</sup>N. W. Ashcroft and N. D. Mermin, *Solid State Physics* (Thomson Learning, 2007).
- <sup>40</sup>T. Dietl, H. Ohno, F. Matsukura, J. Cibert, and D. Ferrand, *Science* **287**, 1019 (2000).
- <sup>41</sup>K. Ando, H. Saito, V. Zayets, and M. C. Debnath, *J. Phys.: Condens. Matter* **16**, S5541 (2004).
- <sup>42</sup>J. Jeffes, in *Encyclopedia of Materials: Science and Technology*, edited by K. J. Buschow, R. W. Cahn, M. C. Flemings, B. Ilschner, E. J. Kramer, S. Mahajan, and P. Veyssi re (Elsevier, Oxford, 2001), pp. 2751–2753.
- <sup>43</sup>F. Walz, *J. Phys.: Condens. Matter* **14**, R285 (2002).
- <sup>44</sup>J. Crangle, *Philos. Mag. A* **5**, 335 (1960).
- <sup>45</sup>E. C. Passamani, E. Baggio-Saitovitch, C. Larica, and S. K. Xia, *Hyperfine Interact.* **83**, 305 (1994).